Progress In Electromagnetics Research C, Vol. 3, 203–214, 2008

ON EXAMINING THE INFLUENCE OF A THIN DIELECTRIC STRIP POSED ACROSS THE DIAMETER OF A PENETRABLE RADIATING CYLINDER

C. A. Valagiannopoulos

School of Electrical and Computer Engineering
National Technical University of Athens
GR 157–73. Zografou, Athens, Greece

Abstract—A thin rectangular dielectric strip is located along the horizontal diameter of a penetrable rod, while the whole structure is illuminated by a plane wave at an arbitrary angle. The unknown field on the slab-sided scatterer is determined by dividing it into a large number of square pixels and thus the problem is solved via analytical integration. A quantity expressing the effect of the strip in the far region is defined and graphically represented with respect to the problem parameters. The attached diagrams are examined and discussed.

1. INTRODUCTION

Infinite dielectric rod of circular shape is a common structure extensively used in modeling electromagnetic devices because it permits simple and analytical treatments. In [1], the imaging of an imperfectly conducting cylinder buried in a three-layer structure by the genetic algorithm is investigated. In [2], a rigorous analysis of scattering by an infinite cylinder coated with metamaterials for a TM or TE normal incident plane wave has been presented in order to achieve low observability. Also in [3], the variation in ionospheric height observed during the dawn or dusk hours is used to develop an electromagnetic imaging system for a cylindrical subterranean formation at extremely low frequencies (ELF).

Finitely or infinitely conducting inclusions inside penetrable cylinders are usually regarded to imitate inhomogeneities of electromagnetic structures. In [4], a metamaterial cylinder which is coated eccentrically by another cylinder with similar characteristic frequencies, scatters an incident wave. In addition, multiple inclusions scattering has been analyzed through a direct method by making use of the T-matrix approach [5]. In [6], a microwave network method has been proposed to derive the solution of a single semicircular channel with several cylindrical inclusions by taking account of multiple scattering effects among parallel channels.

The scattering by rectangular obstacles can be solved approximately (because they do not possess canonical shape, as the cylindrical ones, to be solved rigorously) with insignificant error. This result is achieved via a novel and simple technique presented by Richmond in [7]; the scatterer is divided into a large number of portions whose field is determined by solving a system of linear equations. This method is utilized in [8] where the authors analyze a numerical solution to the 2D scattering problem for a transversely inhomogeneous scatterer located in a stratified medium. Furthermore, in [9] a model describing the antenna radiation over the sea in the presence of two islands is treated through the same technique.

In this work, we study a rectangular dielectric inclusion inside a penetrable circular cylinder posed along its diameter. The structure is investigated under plane wave excitation. The unknown field on this thin dielectric strip is found with Richmond's method by separating it horizontally into numerous square pixels. In this way, the scattering integral is discretized and the response of the structure is readily determined. The proposed methodology have the same characteristics with the one presented in [7]. However, in our approach the scatterer is not surrounded by vacuum; it is embedded into a penetrable cylinder. Various numerical examples are examined where the measured quantity is a function expressing the reaction of the strip into the cylinder called abusively as "transfer function". Some comments on the diagrams justified by physical intuition have been made. It should be stressed that the described technique is applicable to configurations other than the rectangular strip inside the circular cylinder. In particular, it can be easily expanded to treat inhomogeneous inclusions of arbitrary shape, while the host cylinder can have any other canonical shape (e.g., elliptic [10]).

2. DEFINITION OF THE PROBLEM

We consider an infinite dielectric rod of radius A whose center coincides with the origin of the utilized cylindrical coordinate system (ρ, ϕ, z). A rectangular dielectric strip of different material with length $2A$ and height $\xi \ll A$ is posed across the horizontal diameter of the cylindrical formation dividing it into two (upper and lower) semicircular regions as shown in Fig. 1. All the participating materials are magnetically inert with relative dielectric constants ϵ_1 (cylinder, region 1) and ϵ_2 (strip, region 2), while the whole construction exists into vacuum region 0 (ϵ_0, μ_0). The device is excited by a z-polarized plane wave, incident at angle Θ with respect to the horizontal axis, possessing the well-known expansion $E_{0,inc}^{prim}(\rho, \phi) = \sum_{n=-\infty}^{+\infty}(-j)^n J_n(k_0\rho)e^{-jn(\phi-\Theta)}$ [11] where $k_0 = \omega\sqrt{\epsilon_0\mu_0}$ is the free-space wavenumber with a harmonic time dependence $e^{+j\omega t}$. The symbol $J_x(y)$ is used for the cylindrical Bessel function of order x and argument y.

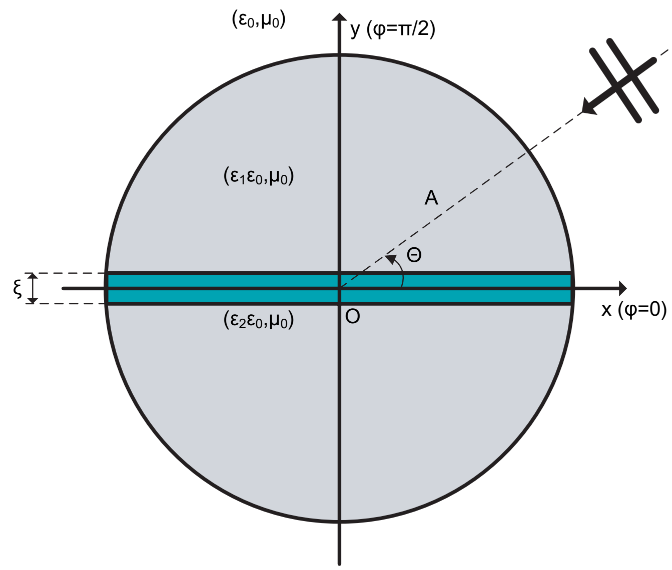

Figure 1. The configuration of the analyzed structure.

The purpose of this study is to investigate the effect of the thin rectangular dielectric strip on the radiation features of a cylindrical rod under the excitation of the plane wave. With a slight loss of generality, we suppose that the length of the strip $(2A)$ is an odd integral multiple of the height ξ, i.e., $A = \frac{2U+1}{2}\xi$ where U is a (relatively large) integer number. In the adopted approach, the rectangular strip will be treated as a "material discontinuity" inside the dielectric cylinder which is considered as the "background configuration". Both the shape and the excitation of the device are invariant across the z axis. Accordingly, the only nonzero electric component is the axial one $E = E_z$ and the problem is reduced to a scalar and two-dimensional one.

The analyzed problem cannot be solved through other semi-analytic techniques; only by purely numerical methods (e.g., FEM).

Consequently, the obtained results can be compared with the corresponding ones produced by measurements or simulations to verify the correctness of the procedures proper implementation. Furthermore, the scattering by incomplete geometries becomes possible through the described methodology. In particular, if one chooses $\epsilon_2 = 1$, one can reliably study the behavior of an aperture formulated between two lunette "D"-shaped dielectric elements.

3. ANALYSIS OF THE STRIP-FREE PROBLEM

3.1. Green's Function

It is well-known that the electric-type Green's function of a two-dimensional problem is defined as the single electric component in each area developed due to the radiation of an elemental dipole of electric current with amplitude $\frac{j}{\omega\mu_0}$ (in Amperes) [12]. The source is placed across the axis ($\rho = P, \phi = \Phi$) inside the dielectric cylinder as the (conditionally removed) strip exists inside its volume. Therefore, the primary component of the Green's function into region 1 is given (for $\rho > P$) by [13]:

$$G_1^{prim}(\rho, \phi, P, \Phi) = -\frac{j}{4} \sum_{n=-\infty}^{+\infty} J_n(k_1 P) H_n(k_1 \rho) e^{-jn(\phi-\Phi)} \tag{1}$$

where $H_x(y)$ is the cylindrical Hankel function of second type.

By utilizing suitable eigenfunction expansions [14] for the Green's functions inside and outside the rod and by applying the necessary boundary conditions [15], one obtains the secondary term of the related quantity into the cylinder:

$$G_1^{sec}(\rho, \phi, P, \Phi) = \sum_{n=-\infty}^{+\infty} F_{G1}(n) J_n(k_1 \rho) J_n(k_1 P) e^{-jn(\phi-\Phi)} \tag{2}$$

In case the observation point (ρ, ϕ) belongs into vacuum region 0, the Green's function takes the form:

$$G_0(\rho, \phi, P, \Phi) = \sum_{n=-\infty}^{+\infty} F_{G0}(n) H_n(k_0 \rho) J_n(k_1 P) e^{-jn(\phi-\Phi)} \tag{3}$$

The series coefficients $F_{G1}(n), F_{G0}(n)$ are defined below:

$$F_{G1}(n) = \frac{j}{4} \cdot \frac{k_0 H_n'(k_0 A) H_n(k_1 A) - k_1 H_n'(k_1 A) H_n(k_0 A)}{k_0 H_n'(k_0 A) J_n(k_1 A) - k_1 J_n'(k_1 A) H_n(k_0 A)} \tag{4}$$

$$F_{G0}(n) = -\frac{1}{2A\pi} \cdot \frac{1}{k_0 H_n'(k_0 A) J_n(k_1 A) - k_1 J_n'(k_1 A) H_n(k_0 A)} \tag{5}$$

3.2. Incident Field

The incident field for the regions 0 and 1 under the excitation of the plane wave, is computed by demanding continuity for the tangential field components across the circular boundary $\rho = A$. Throughout this procedure, the primary quantity is referred to vacuum area contrary to the Green's function determination where the source was contained into the dielectric rod. The related explicit formulas for the axial electric field are readily found.

$$E_{1,inc}(\rho,\phi) = \sum_{n=-\infty}^{+\infty} F_{I1}(n) J_n(k_1\rho) e^{-jn(\phi-\Theta)} \tag{6}$$

$$E_{0,inc}^{sec}(\rho,\phi) = \sum_{n=-\infty}^{+\infty} F_{I0}(n) H_n(k_0\rho) e^{-jn(\phi-\Theta)} \tag{7}$$

The complex coefficients $F_{I1}(n), F_{I0}(n)$ are given by:

$$F_{I1}(n) = -\frac{2j}{A\pi} \cdot \frac{(-j)^n}{k_0 H_n'(k_0A) J_n(k_1A) - k_1 J_n'(k_1A) H_n(k_0A)} \tag{8}$$

$$F_{I0}(n) = -(-j)^n \cdot \frac{k_0 J_n'(k_0A) J_n(k_1A) - k_1 J_n'(k_1A) J_n(k_0A)}{k_0 H_n'(k_0A) J_n(k_1A) - k_1 J_n'(k_1A) H_n(k_0A)} \tag{9}$$

4. ESTIMATION OF THE STRIP EFFECT

4.1. Strip Partitioning

The rectangular region 2 is divided into $(2U+1)$ square pixels of area ξ^2 as $2A = (2U+1)\xi$, each one of which corresponds to a serial number $u = -U, \ldots, U$. In addition, the left side of the leftmost pixel and the right side of the rightmost pixel coincide with the external boundary of the penetrable cylinder because $\xi \ll A$. The center of the u-th part exists on the horizontal axis at distance χ_u from the origin, where $\chi_u = \frac{u}{U}\left(A - \frac{\xi}{2}\right)$. With respect to the used cylindrical coordinate system, the radial distance of the center of the u-th pixel equals $|\chi_u|$, while its azimuthal angle equals $\arg(\chi_u)$. If the size of the square pixels is electrically small, the electric field across each one's area can be considered as constant denoted by $e_2(u) = E_2(\rho = |\chi_u|, \phi = \arg(\chi_u))$. The symbol $p(u)$ defines the area of the u-th part.

4.2. Scattering Theorem

By exploiting the reciprocity of the Green's function, the magnetic inertia of the participating materials and the second Green's integral formula, one can prove the validity of the scattering theorem which in our case is particularized to give:

$$E(\rho,\phi)=E_{inc}(\rho,\phi)+E_{scat}(\rho,\phi)$$
$$=E_{inc}(\rho,\phi)+(k_2^2-k_1^2)\sum_{u=-U}^{U}e_2(u)\iint_{p(u)}G(\rho,\phi,P,\Phi)PdPd\Phi \quad (10)$$

If one applies the aforementioned relations with $(\rho,\phi)\in p(w)$ for $w=-U,\ldots,U$, one obtains the following set of equations:

$$e_2(w)-E_{1,inc}(|\chi_w|,\arg(\chi_w))=(k_2^2-k_1^2)\sum_{u=-U}^{U}e_2(u)M_{wu}$$
$$=(k_2^2-k_1^2)\sum_{u=-U}^{U}e_2(u)\iint_{p(u)}G_1(|\chi_w|,\arg(\chi_w),P,\Phi)PdPd\Phi \quad (11)$$

where $G_1=G_1^{prim}+G_1^{sec}$ is the Green's function of the problem when both the observation (ρ,ϕ) and the source (P,Φ) points belong to region 1.

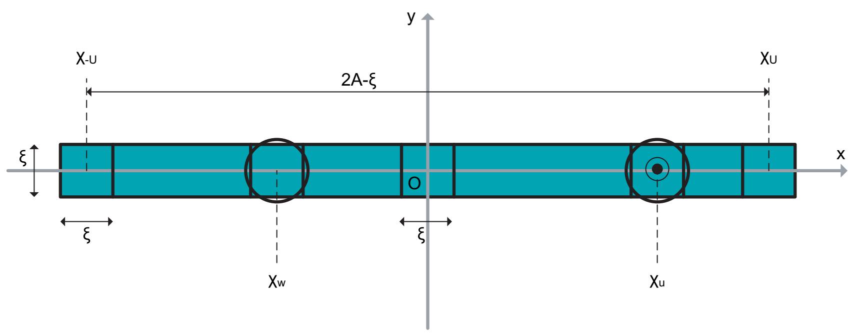

Figure 2. The approximate integration procedure on each pixel. Every square portion comprising the strip is replaced by a circle of equal area.

The primary component of G_1 can be analytically integrated over the representative pixel if the small square region is replaced by a circular one of the same area (having radius $\frac{\xi}{\sqrt{\pi}}$) as shown in Fig. 2. The induced error is very small when ξ is electrically tiny and that is our case. If the expansion (1) is substituted to the integral of (11) and common integrals of Bessel functions [16] are taken into account, we find the expression below:

$$
\begin{aligned}
&\int_{p(u)} G_1^{prim}(|\chi_w|, \arg(\chi_w), P, \Phi) P dP d\Phi \\
&\cong -\frac{j}{2k_1^2} \cdot \begin{cases} k_1\xi\sqrt{\pi} H_0\left(k_1|\chi_w - \chi_u|\right) J_1\left(k_1 \dfrac{\xi}{\sqrt{\pi}}\right), & u \neq w \\ k_1\xi\sqrt{\pi} H_1\left(k_1 \dfrac{\xi}{\sqrt{\pi}}\right) - 2j, & u = w \end{cases}
\end{aligned} \tag{12}
$$

The formula for $u = w$ is derived through a special treatment presented in [7]. As far as the secondary component of the Green's function is concerned, it is slowly varying within the u-th square pixel and thus the related integral is approximated by the function's value on the point $(P = |\chi_u|, \Phi = \arg(\chi_u))$ multiplied with ξ^2.

In this sense, the following $(2U + 1) \times (2U + 1)$ linear system is obtained:

$$
\left[\mathbf{I} - (k_2^2 - k_1^2)\mathbf{M}\right] \bullet \mathbf{e}_2 = \mathbf{e}_{1,inc} \tag{13}
$$

where $\mathbf{I}$ is the $(2U + 1) \times (2U + 1)$ identity matrix, $\mathbf{M}$ is the matrix with elements $M_{wu} = \iint_{p(u)} G_1^{prim}(|\chi_w|, \arg(\chi_w), P, \Phi) P dP d\Phi + \xi^2 G_1^{sec}(|\chi_w|, \arg(\chi_w), |\chi_u|, \arg(\chi_u))$, $\mathbf{e}_2$ is the vector of the unknown values $e_2(w)$ and $\mathbf{e}_{1,inc}$ is the vector of the incident field on the dielectric strip $E_{1,inc}(|\chi_w|, \arg(\chi_w))$ for each $w = -U, \ldots, U$. Mind that when $k_2 = k_1$, the solution of the system is trivial: $\mathbf{e}_2 = \mathbf{e}_{1,inc}$ as there is no "material discontinuity" and the scattering from the homogeneous rod is solely described by the quantity $E_{1,inc}(\rho, \phi)$.

4.3. Transfer Function

The basic function expressing the effect of the dielectric strip on the radiation features of the cylinder is the so-called "transfer function" defined by:

$$
T(\phi, \Theta) = \lim_{\rho \to +\infty} \frac{E_{0,scat}(\rho, \phi)}{E_{0,inc}^{sec}(\rho, \phi)} \tag{14}
$$

The primary component of the incident field does not participate in the aforementioned formula as it simply excites the structure, not revealing its characteristics. For this reason, the denominator equals to the scattering far field of the rod in the absence of the rectangular strip and the numerator to the strip's reaction under the prescribed excitation. The scattered field into vacuum is computed from (10) by considering G_0 as invariant on the area of each small square.

To estimate the field far from the structure, one can exploit the asymptotic expansion of the Hankel function for large arguments: $H_n(\zeta) \sim \sqrt{\frac{2}{\pi\zeta}} e^{-j\left(\zeta - \frac{n\pi}{2} - \frac{\pi}{4}\right)}, \zeta \to +\infty$. Accordingly, the explicit form of $T(\phi, \Theta)$ is readily derived:

$$T(\phi,\Theta) \cong (k_2^2 - k_1^2)\xi^2 \cdot \frac{\sum_{u=-U}^{U} e_2(u,\Theta) \sum_{n=-\infty}^{+\infty} F_{G0}(n) J_n(k_1|\chi_u|) e^{-jn\left(\phi - \arg(\chi_u) - \frac{\pi}{2}\right)}}{\sum_{n=-\infty}^{+\infty} F_{I0}(n) e^{-jn\left(\phi - \Theta - \frac{\pi}{2}\right)}} \tag{15}$$

An extra argument Θ has been added to the function e_2 as the electric field along the strip varies with the incidence angle of the plane wave. One can observe that $T(\phi, \Theta) = 0$ for $k_2 = k_1$, due to the absence of the inhomogeneity.

5. INDICATIVE RESULTS

5.1. Parameters Selection

The value intervals into which the variables of the problem belong should be determined in the first place. The dielectric constants ϵ_1, ϵ_2 possess relatively low values suitable for optical applications (e.g., silicon), while the corresponding materials remain always denser than vacuum: $1 < \epsilon_1, \epsilon_2 < 5$. The radius of the cylinder is chosen moderate, close to the operating wavelength $\lambda_0 = \frac{2\pi}{k_0}$, otherwise the eigenfunction series should have been accelerated with use of Watson transformation [17]. Moreover, the height of the strip ξ is taken many times smaller than the rod's size $2A$, so that the approximate integrations will not induce substantial error. The infinite sums with respect to n in (15) are rapidly converging; as rule of thumb, $N = 15$ terms per wavelength of A are adequate. Due to the symmetry of the structure, the incidence angle varies between the limits: $\Theta \in (0, \pi/2)$.

5.2. Graphs Discussion

In Fig. 3, we present the fluctuation of the transfer function across the forward direction $\phi = \pi + \Theta$ with respect to angle Θ for various permittivities of the strip. The permittivity of the surrounding cylinder is kept fixed $\epsilon_1 = 3$. Mind that the curve corresponding to $\epsilon_2 = 3.1$

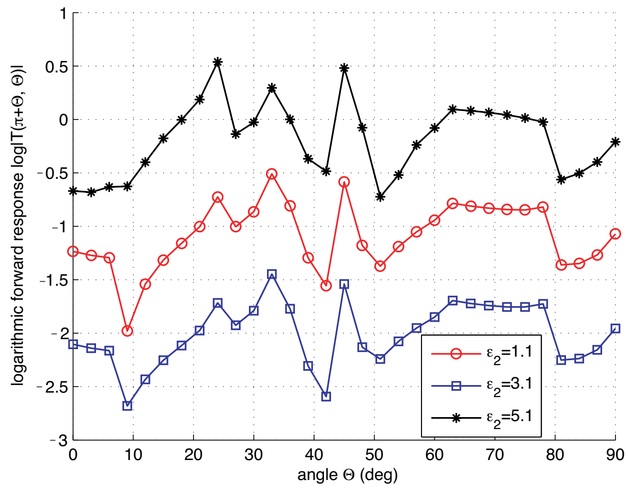

Figure 3. The forward response of the device $\log|T(\pi+\Theta,\Theta)|$ as function of the incidence angle Θ for various strip permittivities ϵ_2. Plot parameters: $A = \lambda_0$, $\epsilon_1 = 3$, $\xi = 2A/51$.

possesses low values as the two dielectrics are similar, while the larger the difference $|\epsilon_1 - \epsilon_2|$ gets, the more substantial is the response of the strip. One can also notice that the shape of the three curves is similar which means that the effect of the angle Θ on the waveforms is almost independent from ϵ_2. For example, a rapid oscillation is remarked close to $\Theta = 45^\circ$ and a relatively invariant behavior within the interval $60^\circ < \Theta < 80^\circ$.

In Fig. 4, we show the variation of the average value of the transfer function around the cylinder $\frac{1}{2\pi}\int_0^{2\pi}|T(\phi,\Theta)|d\phi$ with respect to the permittivity ϵ_2 for several thicknesses ξ of the strip ($\epsilon_1 = 3$). An oblique incidence of the excitation wave $\Theta = \pi/4$ is supposed. Naturally, the response of the rectangular scatterer is proportional to its electrical size, while all the curves take negligible values for $\epsilon_2 = 3$. In addition, the change in the measured quantity is larger for $\epsilon_2 > 3$ (upward sloping) than for $\epsilon_2 < 3$ (downward sloping).

In Fig. 5, a contour plot of the transfer function $|T(\phi,\Theta)|$ along the backward direction $\phi = \Theta$ with respect to the permittivities (ϵ_1, ϵ_2) is depicted. The plane wave is normally incident on the strip ($\Theta = 90^\circ$). The magnitude vanishes for $\epsilon_1 = \epsilon_2$ along the diagonal of the diagram. It is noteworthy that the recorded values are larger on the upper triangle of the graph (where a large maximum is appeared) than the ones of the lower triangle. That means that the response is stronger when $\epsilon_2 < \epsilon_1$ (denser strip's material) than in case $\epsilon_2 > \epsilon_1$.

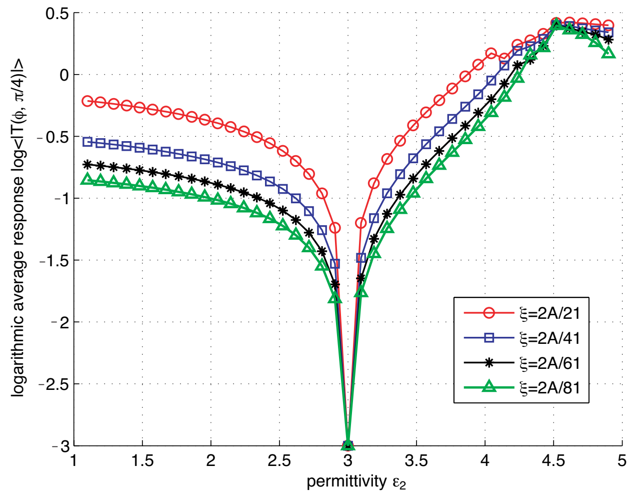

Figure 4. The average response of the device $\log < |T(\phi,\Theta)| >$ as function of the strip permittivity ϵ_2 for various thicknesses of the strip ξ. Plot parameters: $\Theta = \pi/4$, $A = \lambda_0$, $\epsilon_1 = 3$.

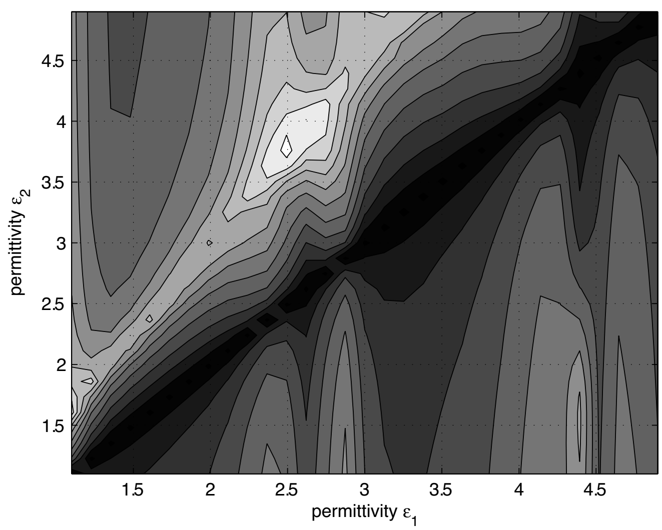

Figure 5. The backward response of the device $|T(\Theta,\Theta)|$ in contour plot as function of the permittivities (ϵ_1, ϵ_2). Plot parameters: $\Theta = \pi/2$, $A = \lambda_0$, $\xi = 2A/51$.

REFERENCES

1. Lee, Y. S., C. C. Chiu, and Y. S. Lin, "Electromagnetic imaging for an imperfectly conducting cylinder buried in a three-layered structure by the genetic algorithm," *Progress In Electromagnetics Research*, PIER 48, 27–44, 2004.
2. Li, C. and Z. Shen, "Electromagnetic scattering by a conducting cylinder coated with metamaterials," *Progress In Electromagnetics Research*, PIER 42, 91–105, 2003.
3. Valagiannopoulos, C. A. and N. K. Uzunoglu, "Scattering of ELF waves by underground formations because of night-day ionospheric ridge," *Radio Science*, Vol. 42, No. RS6S32, 2007.
4. Valagiannopoulos, C. A., "Electromagnetic scattering from two eccentric metamaterial cylinders with frequency-dependent permittivities differing slightly each other," *Progress In Electromagnetics Research B*, Vol. 3, 23–34, 2008.
5. Toyama, H., K. Yasumoto, and T. Iwasaki, "Electromagnetic scattering from a dielectric cylinder with multiple eccentric cylindrical inclusions," *Progress In Electromagnetics Research*, PIER 40, 113–129, 2003.
6. Zhang, Y. J., A. Bauer, and E. P. Li, "A novel coupled T-matrix and microwave network approach for multiple scattering from parallel semicircular channel with eccentric cylindrical inclusions," *Progress In Electromagnetics Research*, PIER 53, 109–133, 2005.
7. Richmond, J. H., "Scattering by a dielectric cylinder of arbitrary cross section shape," *IEEE Transactions on Antennas and Propagation*, Vol. 13, No. 3, 334–341, 1965.
8. Zhuck, N. P. and A. G. Yarovoy, "Two-dimensional scattering from an inhomogeneous dielectric cylinder embedded in a stratified medium: Case of TM polarization," *IEEE Transactions on Antennas and Propagation*, Vol. 42, No. 1, 16–21, 1994.
9. Valagiannopoulos, C. A., "A signal coverage model for two neighboring islands of different size," *Progress In Electromagnetics Research M*, Vol. 2, 115–130, 2008.
10. Khatir, B. N., M. Al-Kanhal, and A. Sebak, "Electromagnetic wave scattering by elliptic chiral cylinder," *Journal of Electromagnetic Waves and Applications*, Vol. 20, No. 10, 1377–1390, 2006.
11. Balanis, C. A., *Advanced Engineering Electromagnetics*, John Wiley and Sons, 595–596, New York, 1989.
12. Valagiannopoulos, C. A., "Semi-analytic solution to a cylindrical microstrip with inhomogeneous substrate," *Electromagnetics*,

Vol. 27, No. 8, 527–544, 2007.

13. Valagiannopoulos, C. A., "Study of an electrically anisotropic cylinder excited magnetically by a straight strip line," *Progress In Electromagnetics Research*, PIER 73, 137–152, 2007.
14. Valagiannopoulos, C. A., "Arbitrary currents on circular cylinder with inhomogeneous cladding and RCS optimization," *Journal of Electromagnetic Waves and Applications*, Vol. 21, No. 5, 665–680, 2007.
15. Valagiannopoulos, C. A., "Closed-form solution to the scattering of a skew strip field by metallic pin in a slab," *Progress In Electromagnetics Research*, PIER 79, 1–21, 2008.
16. Abramowitz, M. and I. A. Stegun, *Handbook of Mathematical Functions*, National Bureau of Standards, 480, Washington D.C., 1964.
17. Valagiannopoulos, C. A., "An overview of the Watson transformation presented through a simple example," *Progress In Electromagnetics Research*, PIER 75, 137–152, 2007.